PAPER

Check for updates

Studying the degradation of bulk PTFE into microparticles *via* SP ICP-MS: a systematically developed method for the detection of F-containing particles†

Raquel Gonzalez de Vega, [ID] *[a] Thebny Thaíse Moro, [ID] [ab] Bernhard Grüner,[ac] Tatiane de Andrade Maranhão,[b] Maximilian J. Huber, [ID] [d] Natalia P. Ivleva, [ID] [d] Etienne Skrzypek,[e] Jörg Feldmann[a] and David Clases [ID] *[f]

Fluoropolymers, such as polytetrafluoroethylene (PTFE), have unique properties, which enable versatile applications in industry and make them useful for various consumer products. However, it is known that these polymers may degrade over time and form small particles with possible implications for the environment and health. Building on previous reports for the detection of fluorine (F) *via* inductively coupled plasma-tandem mass spectrometry (ICP-MS/MS) using a barium-based plasma modifier, this study presents a design of experiments approach (DoE), which optimised plasma parameters, ion optics, mass filtering and collision/reaction cell conditions systematically. The resulting method was capable to detect micro-scaled PTFE particles and to determine number concentrations as well as size distributions. Validation was carried out in two steps: first, micro-scaled PTFE standards were characterised *via* microscopy and Raman spectroscopy and second, carbon-selective single particle (SP) ICP-MS was employed to corroborate results obtained *via* the F-selective method. The developed F-selective method has a high utility to characterise the degradation of bulk PTFE into microplastics, which was demonstrated in a proof-of-concept. Here, bulk PTFE material was stirred in simulated seawater under UV-light illumination for 6 days. After this incubation period, a microplastic number concentration of 2.35×10^5 F-based particles per gram immersed bulk PTFE was detected. PTFE particles had a mean mass and size of 28 pg and 2.7 μm, respectively.

Introduction

Microplastics (MPs, plastic particles in the size range of 1 μm to 1 mm) are increasingly formed and contaminate both the terrestrial and aquatic environment globally. Previous studies have reported that even remote and pristine areas are affected including the deep sea[1] and the polar regions.[2] The origin of MPs is often bulk plastic, which is discharged into the environment and subsequently breaks down into smaller fragments stimulated by weathering and aging effects. In the aqueous environment, seawater is arguably the most relevant matrix and here, plastics may be subjected to constant motion, friction, UV radiation, biological processes as well as complex matrices.[3–5] This accelerates the degradation and fragmentation of plastics and, hence, the formation of small plastic particles. At the current state, methods for the representative and reliable analysis of MPs, especially in the lower size range are still under development limiting endeavours to study their implications for health and the environment.[6–8]

One relevant polymer class is per- or polyfluorinated polyethylene, from which polytetrafluoroethylene (PTFE) is the most prominent. These fluoropolymers are characterised by their strong carbon–fluorine (C–F) bonds. PTFE, like other fluoropolymers, present unique properties with a high utility for diverse applications. For example, PTFE is known for its "non-sticky" behaviour as well as its ability to withstand high temperatures and harsh chemical conditions. These properties make it predestined for various industrial and consumer applications.[9] However, in view of the widespread application of

[a]TESLA-Analytical Chemistry, Institute of Chemistry, University of Graz, Graz, Austria. E-mail: raquel.gonzalez-de-vega@uni-graz.at

[b]Departamento de Química, Universidade Federal de Santa Catarina, Campus Trindade, Florianópolis, Brazil

[c]Institute of Inorganic and Analytical Chemistry, University of Münster, Münster, Germany

[d]Institute of Water Chemistry, Chair of Analytical Chemistry and Water Chemistry, Technical University of Munich, Munich, Germany

[e]Department of Petrology and Geochemistry, NAWI Graz Geocenter, University of Graz, Graz, Austria

[f]NanoMicroLab, Institute of Chemistry, University of Graz, Graz, Austria. E-mail: David.Clases@uni-graz.at

† Electronic supplementary information (ESI) available. See DOI: https://doi.org/10.1039/d4ja00101j

fluoropolymers and the increasing levels of MPs in the environment, we need to understand the degradation of fluoropolymers as well as the formation, distribution, and fate of corresponding MPs.

Several techniques have been suggested for the analysis of MPs including Fourier-transform infrared spectroscopy (FTIR), Raman spectroscopy, thermal analysis and mass spectrometry (MS).[10,11] Especially the latter becomes increasingly relevant and offers unique modes allowing highly selective and sensitive analyses. While molecule-selective methods such as pyrolysis gas chromatography (GC)-MS were described previously,[12–14] the recent advances in elemental mass spectrometry promise new avenues to characterise MPs. A recent relevant method is here inductively-coupled plasma-mass spectrometry (ICP-MS), which can be operated in its "single particle (SP)" mode to count individual particles as well as to establish models on mass- and size distributions.[15] While this method is most commonly used for inorganic nanoparticles, Bolea-Fernandez et al.[16] proposed the detection of MPs via SP ICP-MS by targeting the integral $^{13}C^+$. Laborda et al. subsequently showed that this approach can be used to characterise MPs in consumer products[17] and more recently in river water.[18] Gonzalez de Vega et al.[19] investigated various strategies to improve figures of merits for the detection of MPs in complex matrices, such as seawater, and proposed to target $^{12}C^+$ instead of $^{13}C^+$ to improve the size detection limit. Recently, it was further suggested that SP ICP-MS can be coupled to optical traps and Raman spectroscopy, which allows both the elemental and molecular analysis of single particles.[20] While C is becoming the obvious choice to characterise MPs with elemental mass spectrometry, heteroelements in the polymers may be targeted instead. Especially when targeting fluoropolymers, analysing F would offer a complementary perspective and would be more selective for per- and poly-fluoroalkyl substances (PFAS)-based polymers.

Unfortunately, the direct detection of F by conventional ICP-MS is not possible due to its high first ionisation potential (17.42 eV), which is significantly higher than the first ionisation potential of Ar (12.75 eV). One viable strategy to bypass this issue was introduced by Yamada[21] and is based on the online addition of a Ba solution to the F-containing sample solution. The co-presence of Ba^{2+} and F^- in the plasma allows the formation of BaF^+ (m/z 157) and therefore allows the analysis of the latter as a proxy for F. One limiting factor for this approach is the high abundance of polyatomic interferences (e.g. $^{138}Ba^{18}O^1H^+$, $^{138}Ba^{16}O^1H_3^+$, and $^{138}Ba^{17}O^2H^+$), which however, could be mitigated using a dedicated method for the collision/reaction cell (CRC). Jamari et al.[22] demonstrated that it is possible to use this method in a HPLC-ICP-MS set-up enabling speciation analysis with a high utility for PFAS compounds. Recently, Clases et al.[23] adapted this approach for elemental bioimaging and demonstrated the possibility to map F in biological and geological specimens via LA-ICP-MS. Furthermore, Gelman et al.[24] proved the feasibility of SP ICP-MS to detect F in MPs, which opens new avenues to pinpoint fluoroplastic-based microparticles in the presence of other fluorine-free polymers and even in the presence of dissolved fluorinated molecular compounds.

In this work we systematically investigated and optimised SP ICP-MS of F-based particles using a design of experiment (DoE) approach. To make F analysis via ICP-MS feasible, Ba^{2+} was added as plasma modifier to analyse F as its mass shifted Ba-adduct. For validation, we parallely interrogated PTFE standards via microscopy and Raman spectroscopy and additionally, targeted C for a complementary size distribution model for corroboration. This F-selective method offers opportunities to follow the degradation of bulk PTFE and to consider the generation of small particles in different scenarios. In a proof of concept, we used the F-selective method to investigate the degradation of bulk PTFE in simulated seawater. Seawater is one of the most relevant environmental matrices and we stimulated degradation by immersing bulk PTFE and subjecting it to constant motion and UV radiation.

Materials and methods

An 80 nm Au NP dispersion was bought in 2 mM citrate from nanoComposix (San Diego, CA, USA) and a 3 μm polystyrene-beads MPs standard was obtained from Sigma-Aldrich (St Louis, MO, USA). 3 μm PTFE microparticles with a surface area of 2 m^2 g^{-1} were obtained from Polysciences (Warrington, PA, USA). Upon analysis, stock solutions were sonicated and diluted in containers made of polypropylene for SP ICP-MS. Au, F and Ba elemental standards at 1000 μg mL^{-1} (Single-Element ICP-Standard-Solution Roti®Star) were diluted to working concentrations using ultra-pure water (18.2 MΩ cm, Merck Millipore, Bedford, USA).

To study the degradation of PTFE and the size distribution of resulting particles, bulk PTFE (1.6 g of PTFE septa often used to seal vials) was cut into pieces between 5 and 50 mm^3 and immersed into 50 mL of artificial seawater.[25] A 90 mm diameter round quartz Petri dish without lid was used as container. The mixture was placed under UV light (G8T5 light bulb, 8 watts, 254 nm) at a distance of approximately 7 cm and kept at 21 °C. The PTFE was exposed for 6 days during which evaporated water was refilled with ultra-pure water. After 6 days, the PTFE chunks were visually almost unchanged. Big pieces were removed manually and a cut-off of 15 μm was chosen to avoid the clogging of the nebuliser using a paper filter (VWR®, Qualitative Filter Paper 415). Aliquots of the remaining seawater were collected and analysed to search for PTFE particles. To guarantee the absence of contamination, a blank solution (artificial seawater) without bulk PTFE was prepared under the same experimental conditions and used as control. All seawater samples were diluted 1 : 50 with ultrapure water containing 1.5% Triton X-100 to stabilise PTFE microparticles. The direct analysis of diluted seawater decreased ion transmission and required matrix-matching for accurate size calibration. Blanks, ionic F standard and 3 μm PTFE standard were prepared in diluted seawater to compensate for matrix effects.

For SP detection, an 8900 series ICP-MS/MS system (Agilent Technologies, Santa Clara, CA, USA) was equipped with platinum cones and s-lenses and operated with MassHunter software (Agilent Technologies). A Scott-type double-pass spray chamber was cooled to 2 °C and a MicroMist™ concentric

nebuliser (Elemental Scientific Inc., Omaha, NE, US) was used for sample nebulisation. The inner diameter of the torch's injector was 1.5 mm. The instrument was operated in MS/MS mode and the dwell time of the quadrupole was set to 100 μs. Data analysis was performed using the open-source python-based data processing platform "SPCal".[26] Here, Poisson statistics were used to distinguish ionic background and noise from SP events with an α value of 10^{-3}. The RF power was set to 1.6 kW, the sample depth (z-position) was set to 4.5 mm with a nebulizer gas flow of 1.4 L min^{-1}. Sample uptake rate was calculated gravimetrically to be 0.52 mL min^{-1}. The gradual optimisation to enhance signal to noise ratios and transmission required modification of the plasma, ion optics, quadrupole mass filter and collision/reaction cell (CRC) parameters. A 100 μg mL^{-1} Ba solution was added continuously through a T-piece. One limiting factor in the BaF$^+$ approach was the generation of polyatomic interferences which however, could be mitigated using different gases in the collision/reaction cell (CRC). Here He (99.9999%), H$_2$ (99.9999%) and O$_2$ (20% in argon) were tested in order to evaluate the removal of these interferences while obtaining the best signal to noise ratio (SNR). Optimised parameters are shown in Table 1.

Ionic response factors for Au and F were calculated with ionic standards, and transport efficiencies were calculated using 80 nm Au NPs to be 5.0%. Size calibrations were carried out *via* two different strategies: (1) using the transport efficiency calculated for the Au NPs, (2) Using pre-characterised polystyrene and PTFE standards.

The 3 μm PTFE microparticles standard was further investigated by microscopy and Raman spectroscopy to obtain additional information on purity, shapes and sizes as well as polydispersity. Raman micro-spectroscopy was performed with an alpha 300R (WITec GmbH, Germany) equipped with a Zeiss microscope and a 100× objective (numerical aperture 0.90). The 532 nm emission line of a diode-pumped solid-state laser was used to excite the sample (10 mW on the sample) at room temperature. The Raman scattered light was diffracted on a 600 grooves per mm grating plate and measured with a charge-coupled device camera. Further data analysis was performed with ImageJ software (version 1.54d).[27]

Table 1 Optimised experimental parameters for SP ICP-MS

ICP-MS parameters	Value
Forward power	1600 W
Nebulizer gas	1.4 L min^{-1}
Sample depth	4.5 mm
Extraction 1	−196.5 V
Extraction 2	−5 V
Deflect	5 V
AMU offset (Q_1)	10
AMU gain (Q_1)	130
Energy discrimination	−10 V
Octopole bias	−9.2 V
He	0.8 mL min^{-1}
O$_2$	5%
Axial acceleration	1 V

Design of experiments

For a systematic SP ICP-MS method development, a 3 μm PTFE particle suspension with 1.5% of Triton X-100 was used and various experimental parameters were investigated with the assistance of chemometric tools (Statistica software, version 12.5.192.0). This strategy allowed to carry out a limited number of experiments while still enabling a holistic optimisation of co-dependent instrumental parameters. As such, it was possible to optimise variables rapidly while promoting an understanding of their synergistic effects. To facilitate this approach and to gather a fundamental understanding of the significance of individual parameters, groups of instrumental parameters were interrogated separately and consecutively: (1) plasma parameters; (2) mass filtering parameters (*i.e.*, transmission and resolution); (3) ion optics; (4) CRC parameters.

A response surface method (RSM) with Doehlert design (DD) was used to optimise the instrumental conditions of the plasma and (first) quadrupole. The Doehlert design is usually applied to optimise two variables,[28] which are investigated in three and five experimental levels, respectively. For the plasma optimisation, the variables investigated in three and five levels were sample depth and nebuliser flow, where the experimental conditions investigated were 3.0, 4.5, 6.0 mm, and 1.30, 1.35, 1.40, 1.45, 1.50 mL min^{-1}, for sample depth and nebuliser flow, respectively. The transmission characteristics of the first quadrupole were modulated to tune the mass bandpass and ion flux into the CRC according to strategies previously published by Clases *et al.*[29–32] Briefly, the AMU gain and offset were varied and signal to noise ratios for the BaF$^+$ signal were compared analysing the 3 μm PTFE standard. More information is available in Fig. 1 and the full DD is shown in Table S1.† For the optimisation of the ion optics, extraction lens 1 and 2 as well as the deflect parameters were found to influence signal to noise ratios significantly and therefore, were selected for the DoE approach. Due to the possibility to investigate both factors with 5 experimental levels, a RSM with Central Composite Design (CCD) was chosen to optimise the conditions for "extract 2" and "deflect" lenses. Results are comprised in Table S2 and Fig. S1.† The aim of all optimisations was to achieve the best signal to noise ratios, which was here determined as the ratio of the mean SP signal heights divided by the determined Poisson-based detection threshold.[26]

Due to the high number of parameters that can affect the CRC performance, a 2^5 factorial design (32 experiments) was used as screening method to evaluate the significance of the following variables: octopole bias, energy discrimination, He, H$_2$ and O$_2$ flows (Table S3†). Once concluded, according to the Pareto chart (Fig. S2†) the significant factors ($p < 0.05$) were selected and a RSM with a 3-level Box–Behnken design was further applied to determine the optimal conditions for the significant factors (energy discrimination, O$_2$ and H$_2$ flows). The investigated levels were −5, −10, −15 V; 5, 10, 15%; and 0, 0.5, 1.0 mL min^{-1}, for energy discrimination, O$_2$ and H$_2$ flows, respectively (Table S4 and Fig. S3†).
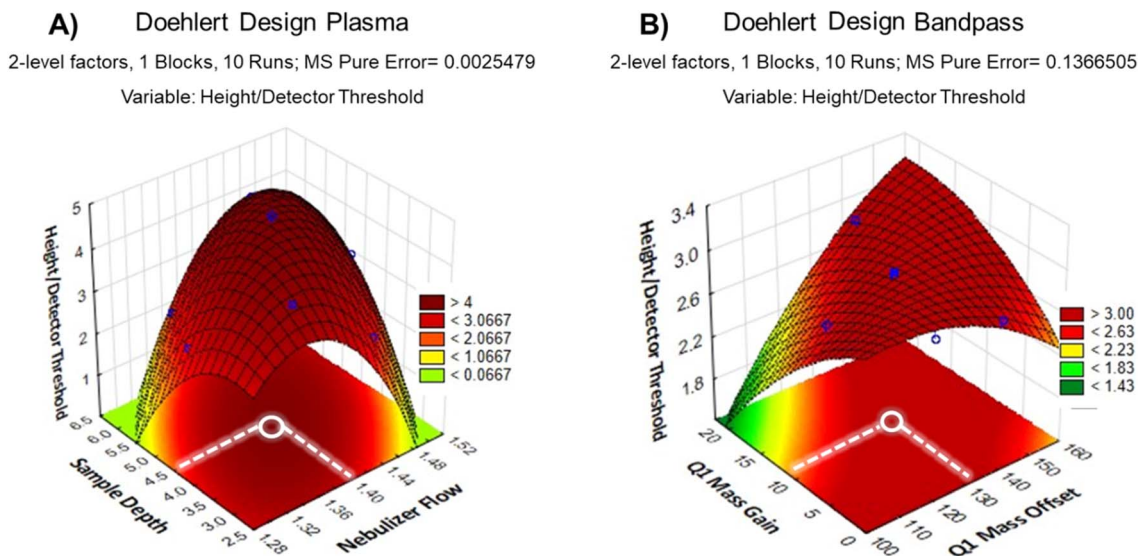
Fig. 1 Colorimetric maps obtained from the Doehlert experimental design for (A) plasma and (B) bandpass optimisations. Selected conditions are marked as a white circle.

Results and discussion

F-selective SP ICP-MS

The generation of F^+ ions in an Ar-based ICP is not viable due to the high first ionisation potential and consequently, the detection of F was originally deemed impossible. However, over the last years, Ba was suggested as plasma modifier, which allows the formation of BaF^+ detectable at m/z 157. It was proposed that this adduct is generated at the narrow intercept of plasma regions containing F^- and Ba^{2+} ions, respectively.[22] The confinement of BaF^+ to a narrow plasma region as well as the high abundance of spectral Ba-based interferences (e.g., $^{138}Ba^{18}O^1H^+$) complicated the method development seeking to find instrumental parameters with optimal signal-to-noise ratios (SNRs). In SP ICP-MS, particles are individually transported into the plasma and following atomisation, elemental cations are formed in discrete ion packages. The transient detection of ions from individual particles allows to distinguish noise and signal events in a single data set and facilitates the calculation of SNRs immensely. Using Poisson statistics ($\alpha = 10^{-3}$), detection thresholds were used as a proxy for noise levels

and compared against the mean signal of SP events in the following. The interdependence of specific instrumental parameters, especially in view of the complex underlying plasma processes, further challenged method development and therefore, conditions were optimised in a design of experiments (DoE)-approach to pinpoint highest SNRs. Instrumental parameters were divided into 4 groups ((1) plasma parameters, (2) ion-optics, (3) mass filter and (4) CRC) and optimised regarding the SNR (or mean SP signal height divided by the detection threshold) individually. To locate the analytical zone containing BaF^+ ions, the torch z-position as well as the nebuliser gas flow were the most relevant plasma-based parameters and a 2-level Doehlert design approach was used to plot SNRs against both parameters (compare Fig. 1A) identifying optimal values of 4.5 mm and 1.4 mL min^{-1}, respectively. Ion extraction and focussing optics were contained in the second group and only hard extraction conditions were found to detect F-based particles. The second extraction voltage and the deflect voltage were found to be interdependent and were optimised using a central composite design approach (Fig. S1 and Table S2†). The third group contained CRC-based parameters
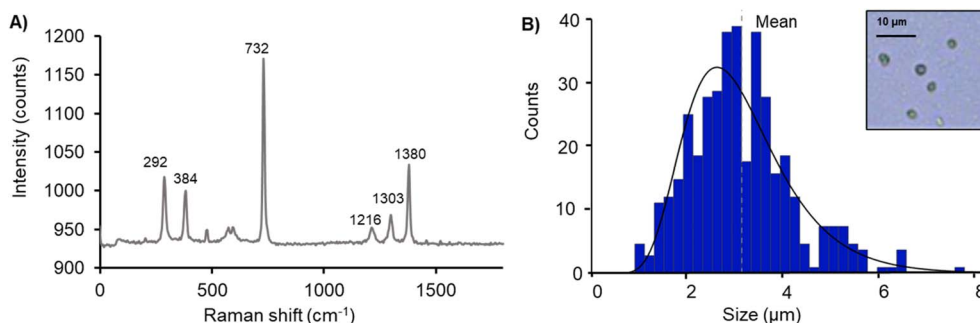

Fig. 2 (A) Raman spectrum obtained from the 3 μm PTFE standard, (B) size histogram and optical image of the detected particles.

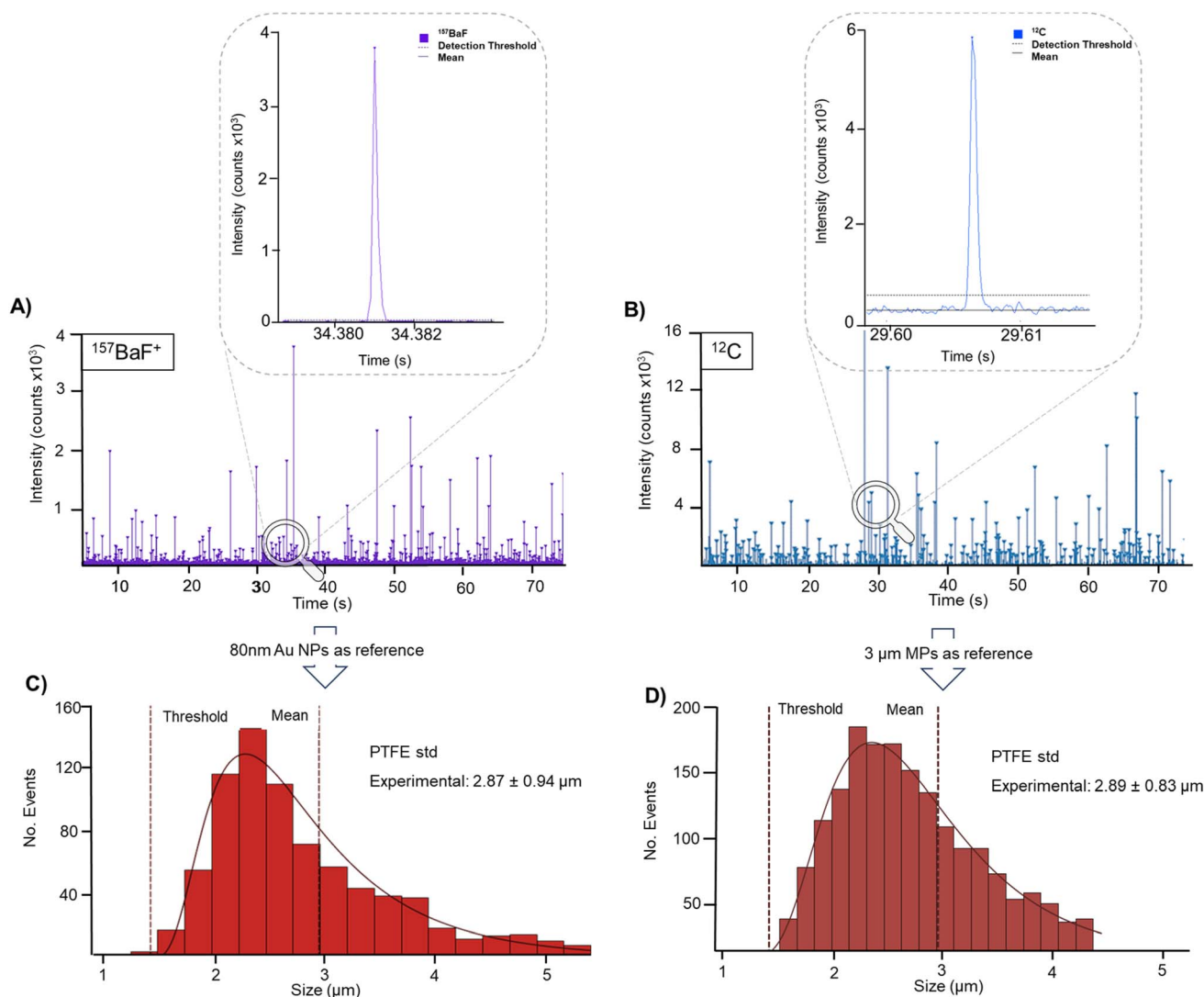**Fig. 3** PTFE standard (3 μm) characterisation *via* F and C SP analysis. (A) and (B) Show SP events detected for $^{157}BaF^+$ and $^{12}C^+$, respectively. A magnification for one selected SP event is provided on the top. (C) and (D) Show the calibrated size distributions, respectively.

including O_2, H_2 and He cell gas flows as well as energy discrimination and the octopole bias, which stipulated reactions as well as kinetic energy discrimination processes to suppress Ba-based interferences. Using a Box–Behnken approach, their independency was investigated and unlike for LA-ICP-MS,[23] here He and H_2 were not found to promote SNRs significantly. In previous work, ICP-MS/MS was found critical to achieve the required selectivity to analyse BaF^+, whereas a recent report showed that also single quadrupole methods are applicable.[24] In this work, the role of the first mass filter was investigated by modulation of the mass bandpass. This was done by manipulating the scanning line of Q_1 which was altering mass resolution and ion transmission by adjusting the tuning parameters "mass offset" and "mass gain" as explained by Clases *et al.*[29–32] A Doerhlert design was used to optimise the Q_1 bandpass systematically as shown in Fig. 1B and a bandpass of 4 amu was found to achieve highest SNR for BaF^+. Optimised values for all remaining parameters as well as more information on the DoE set-up can be found in the ESI.†

Method validation

The accurate calibration of particle sizes as well as the particle transport efficiency relies on the availability of adequate particulate standards. The accuracy for this method was evaluated two-fold. First, micro-scaled PTFE particles were obtained from a commercial source and characterised *via* Raman microspectroscopy prior to SP ICP-MS to ensure the absence of other polymer species and C-based particulates as well as to carry out an optical sizing. Second, a C-selective SP ICP-MS method was used to carry out size calibrations in parallel. Fig. 2A shows a representative Raman spectrum of a 3 μm PTFE standard identified *via* characteristic signature in finger-print regions. The bands at 292 cm^{-1} corresponded to CF_2 twisting, 384 cm^{-1} to CF_2 bending, 732 cm^{-1} to symmetric CF_2 stretching, and 1380 cm^{-1} to symmetric CC stretching.[33,34] In addition, lower intensity bands at 1216 cm^{-1} and 1302 cm^{-1} could represent antisymmetric CF_2 stretching. Evidence for other polymeric impurities were not found. From the optical image, a size
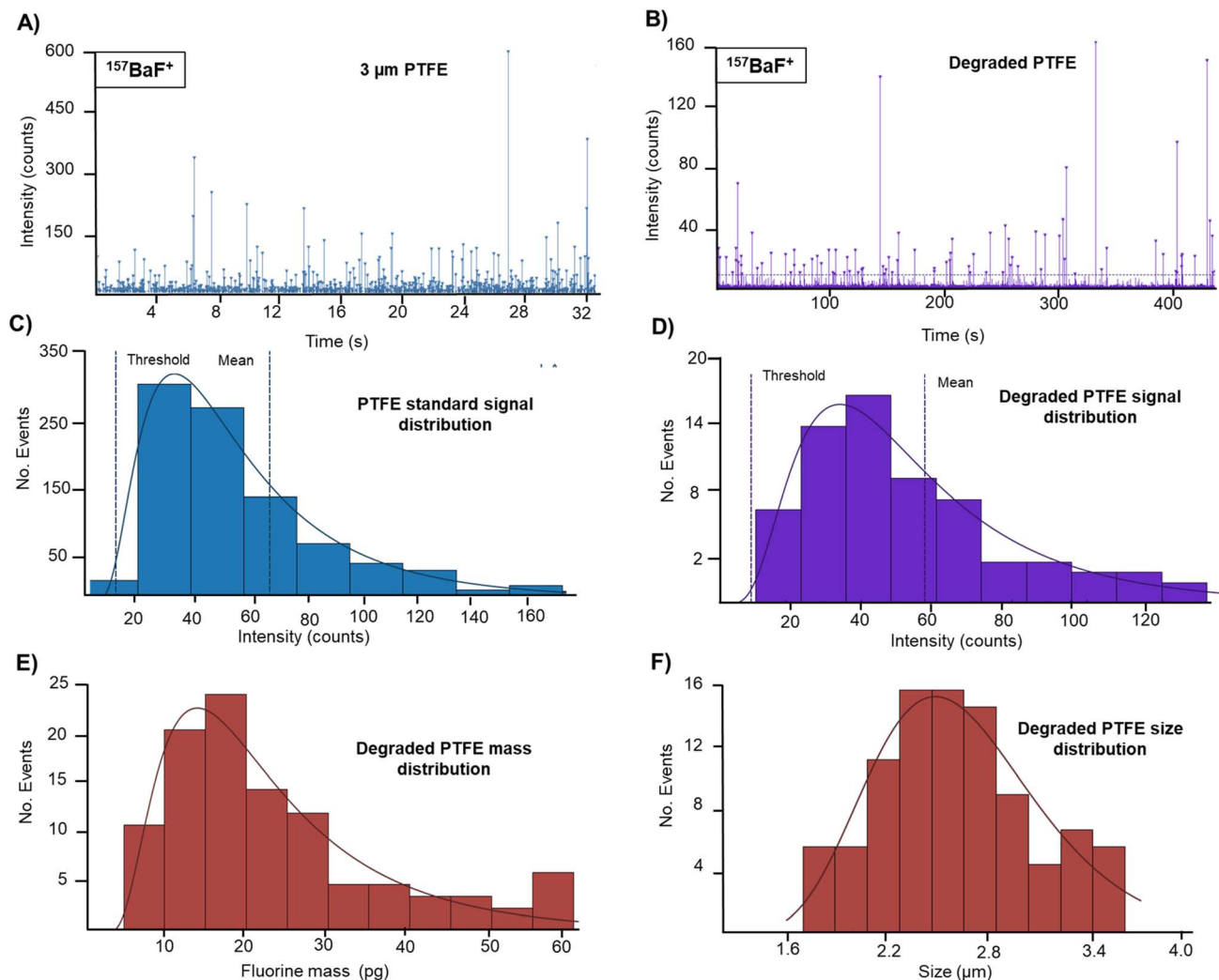
Fig. 4 (A) Raw SP ICP-MS monitoring BaF$^+$ found in the 3 μm PTFE standard suspension. (B) BaF$^+$ ion events detected in a degraded PTFE sample, (C) 3 μm PTFE standard signal distribution, (D) signal histograms from the degraded PTFE sample, (E) histogram representing the fluorine mass (pg) per particle and (F) size histogram (μm) of the detected F-based particles in the degraded PTFE sample.

histogram was created with a lower size cut-off at 1 μm as shown in Fig. 2B. The average particle size was 3.1 ± 1.5.

Subsequently, sizes of PTFE particles were determined with the developed F-selective SP method monitoring the BaF$^+$ adduct. The experimental mean PTFE particle size was 2.9 μm ± 0.9 μm, which was in line with the expected theoretical size of 3 μm. Additionally, size calibrations were carried out targeting C in single PTFE particles *via* SP ICP-MS. The interested reader will find more information on the C-selective method in a previously published study.[19] For the C-selective method, no Triton X-100 was used to limit the mean background signal and consequently, to decrease the C-based size detection limit for MPs. Analysing and calibrating the $^{12}C^+$ signal, an average PTFE particle size of 2.9 ± 0.8 μm was determined. Fig. 3A and B show both the raw BaF$^+$ and ^{12}C signals, respectively, and Fig. 3C and D show the calibrated size distributions. For the F-selective method, the size detection limit of PTFE particles was determined to be 1.1 μm. At particles sizes above 15 μm, nebuliser

clogging occurred frequently and filter paper with a cut-off of 15 μm was used to remove larger particles and agglomerates. Compared to a previous report, the lower detection limit was increased,[24] which was likely due to a more conservative approach to define the detection threshold in this study. As size detection limits for PTFE particles using the C-selective method were lower,[19] a manual decision limit was set to the F-based size detection limit to enable a direct comparison of the mean size and size distribution. Both the F and C-selective methods determined similar mean values and standard deviations (2.9 ± 0.9 μm and 2.9 ± 0.8 μm, respectively) and were furthermore in line with the optical sizing approach (3.1 ± 1.5 μm).

Application to environmental samples: a proof of concept

Pollution of seas and oceans by plastic waste with dimensions across the nano-, micro and visible scale may pose a threat to marine health. It is known that plastics gradually degrade in the environment and form micro- and nano-scaled particles, which

can be found ubiquitously and consequently raise increasing concerns. SP ICP-MS is a powerful method to count individual particles at high rates and to model mass and size distributions. However, so far it has not been employed to study the degradation of PTFE. The here developed F-selective method was used to characterise the formation of PTFE microparticles in an environmental context and here, bulk PTFE was incubated in a simulated seawater matrix and irradiated with UV light. Seawater was selected as one of the most relevant and abundant environmental matrices for plastics. A control without bulk PTFE was set up identically and did not show any F-based SP signals when analysed *via* SP ICP-MS. After an incubation time of six days, the F-selective SP ICP-MS method was used to investigate the number and size of microparticulate PTFE. In view of the complex matrix, which was not immediately compatible with ICP-MS, samples were diluted (1 : 50) and an aerosol dilution set-up was employed as reported previously[19] allowing robust analysis over an extended period. For calibration, PTFE particles previously characterised optically, *via* targeting C and *via* targeting F were dispersed in simulated seawater for matrix-matching and analysed as standard for immediate size calibration using the mass-responses, respectively. Fig. 4A shows the analysis of the 3 μm sized PTFE standards in simulated seawater. Fig. 4B shows the transient analysis of the degraded sample after the removal of visible bulk PTFE indicating the presence of micro-scaled PTFE. Fig. 4C and D show the signal histogram of the sample and standard, respectively. The mean response for the 3 μm sized standard was used to calibrate the PTFE mass and size distributions as shown in Fig. 4E and F. The mean mass and size were 28 pg and 2.7 μm, respectively. The particle number concentration (PNC) obtained for micro-PTFE was 2.35×10^5 F-based particles per gram immersed bulk PTFE.

It is worth mentioning that SP ICP-MS cannot distinguish F-based particles containing different species and that mass and size models are restricted to particles with known density and F-mass fraction. While this is the case for targeted degradation experiments, real and unknown environmental samples may contain other F-based species challenging current approaches. One way to address this issue is an additional characterisation *via* a complementary (molecule-selective) particle detection paradigm. For example, previous Raman analysis coupled online to SP ICP-MS may offer a viable solution as recently demonstrated for polystyrene particles.[20]

Conclusions

MPs and fluoropolymers present significant challenges for the development of analytical methods due to their complexity, diversity, and elusive nature. This work focused on the systematic development of a F-selective SP ICP-MS method for the analysis of PTFE. Here, Ba was used as plasma modifier to stimulate the formation of BaF^+, which can be targeted at *m/z* 157. Using a DoE-approach, optimal conditions for plasma, ion optics, quadrupole and CRC were determined. The developed SP ICP-MS method was validated using optical methods and by targeting C in individual PTFE microparticles additionally. In

a proof-of-concept, bulk PTFE was artificially degraded in simulated seawater and subjected to constant motion and UV radiation. Mass and size calibration was performed by analysing previously characterised PTFE standards suspended in the simulated seawater. The presented SP ICP-MS method expands the analysis of fluoroplastic microparticles by targeting both C and F and enables the determination of number and size distribution even in complex matrices such as seawater.

Data availability

The data supporting this article have been included as part of the ESI.†

Conflicts of interest

The authors declare no conflicts of interest.

Acknowledgements

References

1 L. Van Cauwenberghe, A. Vanreusel, J. Mees and C. R. Janssen, *Environ. Pollut.*, 2013, **182**, 495–499.

2 H. Emberson-Marl, R. L. Coppock, M. Cole, B. J. Godley, N. Mimpriss, S. E. Nelms and P. K. Lindeque, *Front. Mar. Sci.*, 2023, **10**, 1241829.

3 J. A. Ivar Do Sul and M. F. Costa, *Environ. Pollut.*, 2014, **185**, 352–364.

4 A. Ter Halle, L. Ladirat, X. Gendre, D. Goudouneche, C. Pusineri, C. Routaboul, C. Tenailleau, B. Duployer and E. Perez, *Environ. Sci. Technol.*, 2016, **50**, 5668–5675.

5 F. Cheng, T. Zhang, Y. Liu, Y. Zhang and J. Qu, *J. Xenobiot.*, 2022, **12**, 1–12.

6 Y. Li, L. Tao, Q. Wang, F. Wang, G. Li and M. Song, *Environ. Health*, 2023, **1**, 249–257.

7 D. Katyal, E. Kong and J. Villanueva, *Environ. Health Rev.*, 2020, **63**, 27–31.

8 H. Dong, X. Wang, X. Niu, J. Zeng, Y. Zhou, Z. Suona, Y. Yuan and X. Chen, *TrAC, Trends Anal. Chem.*, 2023, **167**, 117241.

9 S. H. Korzeniowski, R. C. Buck, R. M. Newkold, A. El kassmi, E. Laganis, Y. Matsuoka, B. Dinelli, S. Beauchet, F. Adamsky, K. Weilandt, V. K. Soni, D. Kapoor, P. Gunasekar, M. Malvasi, G. Brinati and S. Musio, *Integr. Environ. Assess. Manage.*, 2023, **19**, 326–354.

10 S. Primpke, S. H. Christiansen, W. Cowger, H. De Frond, A. Deshpande, M. Fischer, E. B. Holland, M. Meyns, B. A. O'Donnell, B. E. Ossmann, M. Pittroff, G. Sarau, B. M. Scholz-Böttcher and K. J. Wiggin, *Appl. Spectrosc.*, 2020, **74**, 1012–1047.

11 N. P. Ivleva, *Chem. Rev.*, 2021, **121**, 11886–11936.

12 L. Hermabessiere, C. Himber, B. Boricaud, M. Kazour, R. Amara, A. L. Cassone, M. Laurentie, I. Paul-Pont, P. Soudant, A. Dehaut and G. Duflos, *Anal. Bioanal. Chem.*, 2018, **410**, 6663–6676.

13 Y. Xu, Q. Ou, X. Wang, F. Hou, P. Li, J. P. van der Hoek and G. Liu, *Environ. Sci. Technol.*, 2023, **57**, 3114–3123.

14 R. Gonzalez de Vega, M. Plassmann, D. Clases, K. Zangger, V. Müller, E. Rosenberg, A. Reimann, L. Skedung, J. P. Benskin and J. Feldmann, *Anal. Chim. Acta*, 2024, **1314**, 342754.

15 M. Resano, M. Aramendía, E. García-Ruiz, A. Bazo, E. Bolea-Fernandez and F. Vanhaecke, *Chem. Sci.*, 2022, **13**, 4436–4473.

16 E. Bolea-Fernandez, A. Rua-Ibarz, M. Velimirovic, K. Tirez and F. Vanhaecke, *J. Anal. At. Spectrom.*, 2020, **35**, 455–460.

17 F. Laborda, C. Trujillo and R. Lobinski, *Talanta*, 2021, **221**, 121486.

18 C. Trujillo, J. Pérez-Arantegui, R. Lobinski and F. Laborda, *Nanomaterials*, 2023, **13**, 1582.

19 R. Gonzalez de Vega, S. Goyen, T. E. Lockwood, P. A. Doble, E. F. Camp and D. Clases, *Anal. Chim. Acta*, 2021, **1174**, 338737.

20 C. Neuper, M. Šimić, T. E. Lockwood, R. Gonzalez de Vega, U. Hohenester, H. Fitzek, L. Schlatt, C. Hill and D. Clases, *Anal. Chem.*, 2024, **96**, 8291–8299.

21 N. Yamada, *Agilent 8800 ICP-QQQ Appl. Handbook*, Agilent Technologies, 2013, pp. 33–34.

22 N. L. A. Jamari, J. F. Dohmann, A. Raab, E. M. Krupp and J. Feldmann, *J. Anal. At. Spectrom.*, 2017, **32**, 942–950.

23 D. Clases, R. Gonzalez de Vega, J. Parnell and J. Feldmann, *J. Anal. At. Spectrom.*, 2023, **38**, 1661–1667.

24 F. Gelman, M. Muszynska, J. Karasinski, O. Lev and L. Halicz, *J. Anal. At. Spectrom.*, 2022, **37**, 2282–2285.

25 D. R. Kester, I. W. Duedall, D. N. Connors and R. M. Pytkowicz, *Limnol. Oceanogr.*, 1967, **12**, 176–179.

26 T. E. Lockwood, R. Gonzalez De Vega and D. Clases, *J. Anal. At. Spectrom.*, 2021, **36**, 2536–2544.

27 W. S. Rasband, *ImageJ*.

28 U. M. F. M. Cerqueira, M. A. Bezerra, S. L. C. Ferreira, R. de Jesus Araújo, B. N. da Silva and C. G. Novaes, *Food Chem.*, 2021, **364**, 130429.

29 D. Clases, *J. Anal. At. Spectrom.*, 2023, **38**, 2518–2527.

30 S. Meyer, R. Gonzalez de Vega, X. Xu, Z. Du, P. A. Doble and D. Clases, *Anal. Chem.*, 2020, **92**, 15007–15016.

31 M. Horstmann, R. Gonzalez de Vega, D. P. Bishop, U. Karst, P. Doble and D. Clases, *J. Anal. At. Spectrom.*, 2021, **36**, 767–775.

32 D. Clases, R. Gonzalez de Vega, S. Funke, T. E. Lockwood, M. T. Westerhausen, R. V. Taudte, P. A. Adlard and P. A. Doble, *J. Anal. At. Spectrom.*, 2020, **35**, 728–735.

33 T. Shimoaka, M. Sonoyama, H. Amii, T. Takagi, T. Kanamori and T. Hasegawa, *J. Phys. Chem. A*, 2017, **121**, 8425–8431.

34 S. Lee, K.-K. Kang, S.-E. Sung, J.-H. Choi, M. Sung, K.-Y. Seong, J. Lee, S. Kang, S. Y. Yang, S. Lee, K.-R. Lee, M.-S. Seo and K. Kim, *Polymers*, 2022, **14**, 2220.

This journal is © The Royal Society of Chemistry 2024

J. Anal. At. Spectrom., 2024, **39**, 2030–2037 | **2037**